

26th CIRP Life Cycle Engineering (LCE) Conference

# Porous metal bonds increase the resource efficiency for profile grinding II

Berend Denkena<sup>a</sup>, Thilo Grove<sup>a</sup>, Marc-André Dittrich<sup>a</sup>, Vino Suntharakumaran<sup>a\*</sup>

<sup>a</sup>*Institute of Production Engineering and Machine Tools, Leibniz University Hannover, An der Universität 2, 30823 Garbsen, Germany*

\* Corresponding author. Tel.: +49-511-762-18274; fax: +49-511-762-5115. E-mail address: [suntharakumaran@ifw.uni-hannover.de](mailto:suntharakumaran@ifw.uni-hannover.de)

## Abstract

Profile grinding is irreplaceable for the machining of various brittle and hard workpieces such as cutting tools, i.e. milling and boring tools, seal components made off ceramic as well as bearing components. Regarding the required energy for the machining of one volume element, grinding is inefficient compared to other manufacturing processes. By using grinding wheels with a porous metal bond and grains that tend to splinter the process forces can be reduced without influencing the tool wear. This allows for increasing the material removal rate while keeping the process forces on a constant level, ultimately reducing the energy consumption per workpiece manufactured. This paper focuses on the correlation between material removal rate, energy consumption, process temperatures and forces as well as the material removal mechanisms for the profile grinding of cemented carbide.

© 2019 The Authors. Published by Elsevier B.V. This is an open access article under the CC BY-NC-ND license

(<http://creativecommons.org/licenses/by-nc-nd/3.0/>)

Peer-review under responsibility of the scientific committee of the 26th CIRP Life Cycle Engineering (LCE) Conference.

*Keywords:* Resource Efficiency; Profile Grinding; Brittle Materials; Metal Bond

## 1. Introduction

Grinding is irreplaceable for the machining of many, especially brittle-hard materials such as carbide or ceramic. Thus, cutting tools such as milling or drilling tools, sealing components made of ceramic or components made of quartz glass for the semiconductor industry are often ground [1,2, 3]. In those applications, profile grinding, which is characterized by comparatively high removal rates, is of particular importance [4, 5]. In terms of the energy required to cut a volume element, however, grinding is inefficient compared to other manufacturing processes [6]. By using more efficient machine components and an adapted coolant supply, the energy consumption of the machining process may be reduced [7, 8]. However, these approaches are often associated with large investments for existing production facilities since entire machines or individual components must be replaced. An increase in the productivity of the grinding process, however, can be achieved quickly and inexpensively. It is possible by selecting suitable grinding wheel specifications leading to reduced energy consumption per manufactured component.

## 2. Motivation, aim and approach

Within the metalworking industry, machine tools are the main consumers of electrical energy with over 66% of the overall energy demand. This highlights the opportunity to save energy and reduce costs in this field. The energy demand during grinding is characterized by several aspects. One possible strategy in order to reduce the total amount of energy required in grinding is to increase the productivity of the process. Thus, less time is needed to machine a workpiece while maintaining a high quality. For example, energy-intensive auxiliary units such as coolant pumps, cooling, hydraulics and cooling lubricant preparation, which in some cases consume more than 75% of the required energy of a machine tool, are running for shorter time intervals [9]. A tool that generates low mechanical and thermal workpiece loads with the same material removal rate separates the material more efficiently than a tools that generate higher loads. It offers the potential to machine components in less time without adversely affecting the generated workpiece quality [10]. This paper aims

for presenting possibilities for the selection of productive grinding tools on the basis of the mechanical and thermal load on the workpiece during grinding. In order to reach this goal, the material separation mechanism, the generated process heat and the spindle power required for machining are examined.

### 3. Experimental setup

A Walter Helitronic Vision 400L grinding machine has been used for all experiments. Cemented carbide specimen with the specification “KXF” measuring 10×20×100 mm have been machined primarily by creep-feed grinding. In each grinding experiment three passes with a width of cut of  $a_p = 5$  mm were ground resulting in a material removal of 540 mm<sup>3</sup>/mm. The creep-feed grinding process has been chosen in order to simulate the thermal loads while profile grinding without having to implement complicated profiles. A cylindrical 1A1-grinding wheel geometry was used. In all experiments porous metal bonded grinding wheels, called “Paradigm”, with diamond grains have been used. A DDS-form roller was used to dress the grinding wheels mechanically. This dressing tool consists of CVD-cutting particles implemented into a sintered multilayer bond. All grinding wheels were dressed with a overlapping rate of  $U_d = 12$ , a depth of dressing cut  $a_{ed} = 1$  μm and a ratio of dressing speeds  $q_d = 0.8$  in order to set the grinding wheel topography a vitrified corundum sharpening bock was used. The grinding wheels are sharpened with a cutting speed of  $v_c = 20$  m/s, feed rate  $v_f$  of 100 mm/min and a depth of cut  $a_{es} = 1$  mm. The different grinding wheel specifications are shown in table 1.

Table 1: Grinding wheel specifications used for the investigations

Tool	Grain size [μm]	Concentration C [-]	Grain type	Porosity [%]
1	54	150	Splintering	38
2	30	150	Splintering	38
3	76	150	Splintering	38
4	54	176	Splintering	38
5	54	150	Blocky	38
6	54	150	Splintering	46

The topographies of the investigated grinding wheel specifications were characterized. In this case imprints of the grinding wheel topography by means of casting compounds were taken and the hardened impressions were scanned with a 3D profilometer “μScan” from the company nanofocus.

In order to evaluate the load on the grinding wheel and workpiece the spindle load was tracked simultaneously to the grinding process. The process forces were measured with a three component dynamometer from Kistler in order to evaluate the mechanical load. The model with the number 9257B was used allowing for measuring forces in x, y and z direction in the positive and negative range of 5.000 N.

By measuring the process temperature it is possible to evaluate the thermal loads on the workpiece and the grinding wheels. The experimental setup is shown in Figure 1. Calibrated thermocouples of the type K with a probe length of 150 mm and a probe diameter of 0.5 mm from the company

RS Components GmbH were placed in holes that were eroded into the carbide workpieces. The sampling rate was set at 12.5 Hz. The amplification of the signal takes place by using a measurement amplifier from the company Bedo Elektronik GmbH with signal connection cards from the type 12 before the signal is transmitted to the measuring computer. The used measurement technology allows for the measurement of eight temperatures at the same time. In case of the temperature measurement it is important to correct the measured temperature. The deviation of the correction factor from the value one in the case of the thermocouples used is in the thousandth range and thus negligible. With a depth of cut of 1.8 mm, the process temperatures were recorded at a distance of 0.7 mm from the workpiece surface. The mean contact zone temperature is calculated based on temperature models. The basis for calculating the surface temperature during grinding is based on the approach of Carslaw and Jaeger [12] [13] [14]. Consequently, the approach of Takazawa is applied due to the high complexity of solving the integral calculation according to Göttsching [15]. This approach determines the two-dimensional temperature distribution at defined depths  $z$  below the workpiece surface via an approximation formula. First, the heat dissipation factor  $K_w$ , which is calculated from the thermal conductivity  $\lambda_w$ , the density  $\rho$  and the heat capacity  $c_p$  of the machined carbide (KXF) and tool, in this case represented by the grain material (diamond), are calculated. The factor  $K_w$  is consequently calculated to 35%. The calculated factor  $K_w$  and state of the art standard set of tables allow for the calculation of a value of 340 °C. This means that the measured temperature at a depth of 0.7 mm increases on average by approx. 340 °C to the surface. The absolute values of the temperatures increase, but the relative relation to each other remain untouched [16].

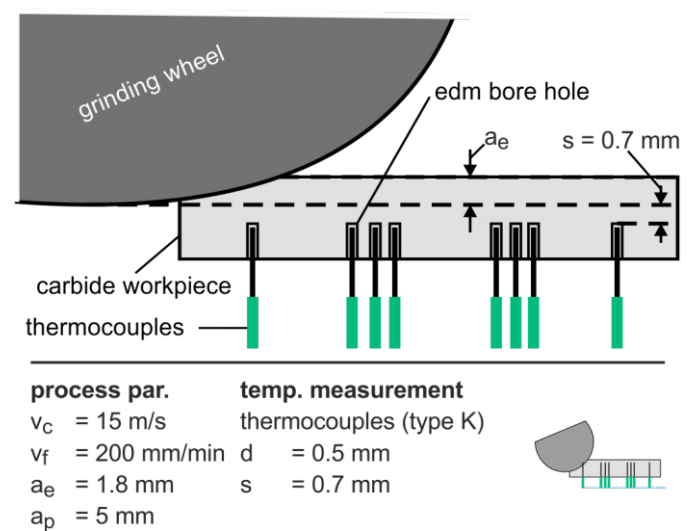


Figure 1: experimental set up in order to measure process temperatures while grinding

An investigation of the workpiece surfaces after separating tool and workpiece during the grinding process with the aid of a quick-stop device allows for the correlation of the aforementioned process loads with the material deformation mechanism. The type of material separation can be determined providing information regarding the qualitative share of

mechanical and thermal loads on the given grinding wheel specification.

#### 4. Choosing grinding wheel specifications according to the impact on resource efficiency

A high pore volume of the grinding wheel ensures an improved coolant supply into the contact zone and an increased chip evacuation. There is less friction in the grinding process and thus less energy consumption for mechanical and thermal workpiece loads. Conventional grinding wheels with a vitrified bond have a high pore volume. In case of these tools, the wear increases with increasing pore volume. This results in a lower profile accuracy in the process and eventually of the workpiece. Conventional metal bonds, however, have a higher profile retention, but a low pore volume. A novel highly porous metal bond combines the advantages of vitrified and metal bonded grinding wheels. The abovementioned types of bonds are shown on scanning electron micrographs in Figure 2.

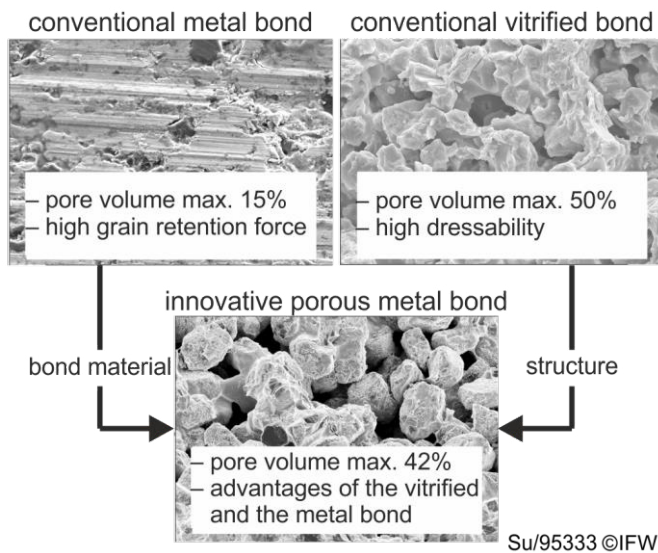


Figure 2: Comparison of various bond systems

The porous metal bond is structurally similar to the porous ceramic bond, the conventional metal bond has the previously described dense structure. The increase in productivity during grinding can be realized in the case of porous metallic bonds both by the use of abrasive grains that are likely to splinter and by a high porosity in the grinding tool. Grinding tests at the Institute of Production Engineering and Machine Tools (IFW) of the Leibniz University of Hannover show that the process forces are reduced by the porous metal bond and grains with excellent friability. The grinding wheel wear is not affected negatively [17]. In this way, the material removal rate can be increased and the energy consumption per manufactured component can be reduced.

##### 4.1. Spindle load as a measure of the tool load in tangential direction

The spindle load is a measure of the loading of the grinding tool in the tangential direction of the tool engagement. It is the share of the effective power in the maximum power of the drive spindle. Modern machine tools are able to record these signals

during the machining process. In the present case, the material removal rate is gradually increased and grinding tools of different specifications are examined. Based on the reference tool number one with 54  $\mu\text{m}$  diamond grits with high friability, a grain concentration of C150 and a bond porosity of 38%, the individual specifications mentioned were varied. The results are shown in Figure 3. The grinding tool number two with D30 grains has macroscopic cracks and shows clogging at a removal rate of 6  $\text{mm}^3/\text{mms}$ . The main reason for this type of wear lies in the comparatively low chip space of this grinding wheel specification. This leads to less available space for removed material and cutting fluid supply. Increased friction leads to higher thermal loads, clogging also increased the mechanical loads. This ultimately leads to the generation of cracks on the circumferential surface of the grinding wheel. Thus, this grinding wheel specification exceeds the abort criterion of the investigations and will not be considered further. This limit was also reached by the grinding wheel number five with a block shaped diamond type and by the tool number three with a D76 grain specification.

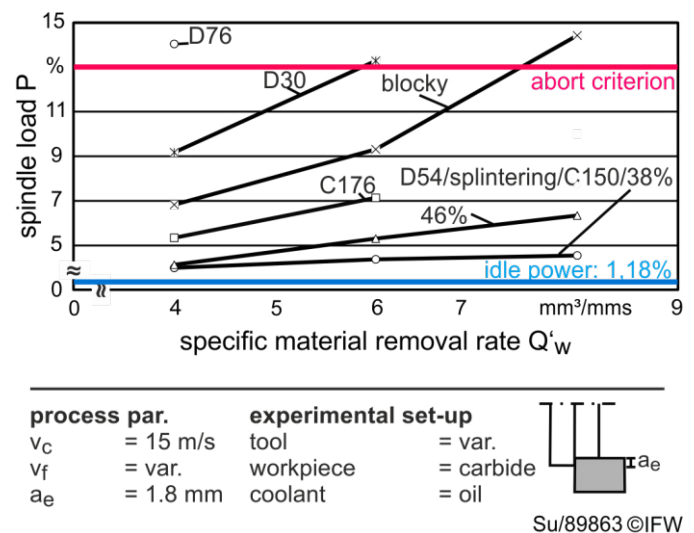


Figure 3: Spindle load depending on the material removal rate and the grinding wheel specification

##### 4.2. Analysis of the grinding wheel topography

In order to identify the cause of the low material removal rate of the grinding wheel number three with a D76 grain, it is necessary to characterize the topography of this grinding wheel specification. Initially, the results presented in Figure 4 provide a qualitative image of the existing chip space for grinding wheels with different grain sizes but identical dressing. In a second step, material ratio curves (Abbott curves) can be determined. They provide values of reduced peak heights ( $R_{pk}$ ), which in turn correlate with the grain protrusion. Increased valley depths ( $R_{vk}$ ) can be associated with a lack of grain retention. The grain protrusion affects the process forces by providing more or less space for the flow of material, resulting in friction between bond and workpiece and increased process forces. The mean grain protrusion is defined by Wunder as the material height at 90% of the material of a material ratio curve. It corresponds approximately with the mean depth of the



profile valleys below the core region of the material ratio curve [11].

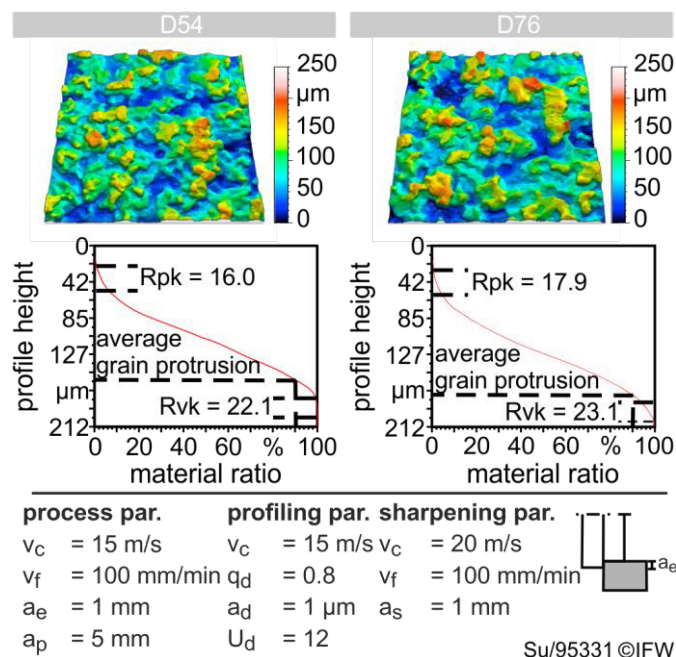


Figure 4: Topography scans based on casting compounds for evaluating the chip space before grinding

In the case of the grinding wheel number three with a larger D76 grain size it is approximately 18 µm higher and corresponds to the size difference of the two investigated grain sizes. In principle, a larger chip space is available, which enables high removal rates and improved tool life. However, the qualitative pictures in Figure 4 show, that the number and retention of the D76 abrasive grains is lower than that of the reference tool number one with D54 abrasive grains. The reduced grain embedding is quantified by the higher Rvk value compared to the D54 grain size. If the grain concentration remains constant, a change in size is possible only by changing the number of grains. The individual less strongly embedded D76 grains, are therefore loaded stronger and splinter or break out during the grinding process. Consequently, there are less abrasive grains available for the grinding process. This in turn leads to an increasing tendency for bond friction, which is validated by the highest measured spindle load of the test series. In this case, the material removal rate is not increased further in order to avoid damage of the engaging partners.

#### 4.3. Process forces as a measure of the tool load in normal direction

An increased load on the grinding tool in the tangential direction of action can not categorically be rated positive or negative. In principle, the same cutting volume is removed in each case, but a high tangential load can either indicate an efficient material separation or an overload of the grinding tool. In combination with the load in the normal direction of the tool, however, an evaluation regarding the efficiency of the present process is possible. The blocky grains for example generate a

high spindle load, but only a moderate mechanical load in the normal direction, as presented in Figure 5.

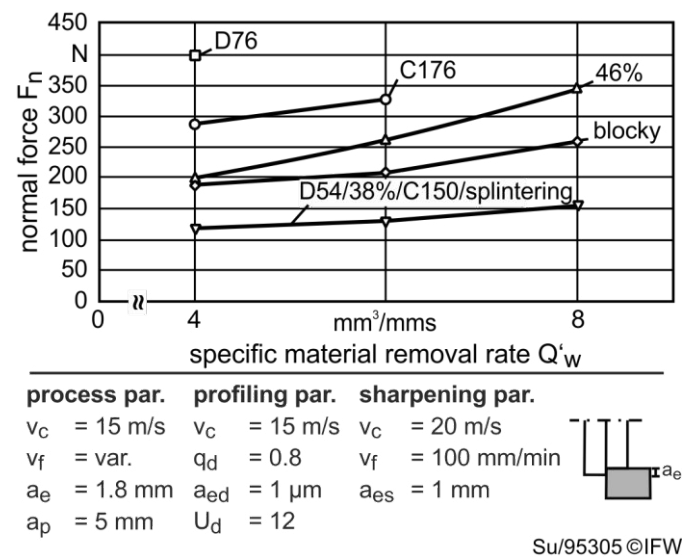


Figure 5: Process force in normal direction depending on the material removal rate and the grinding wheel specification

At this point, a consideration of the present material separation mechanism is necessary. The grinding tool number four with a grain concentration of C176 could not be used beyond a material removal rate of 6 mm³/mms, but generates a comparatively low spindle load. However, the generated normal force is the highest right after the tool number three with a D76 grit and indicates a mechanical overload of the grinding tool. This implies high process friction and thermal stress on the active partners. The tool number six with a porosity of 46% has the same behavior.

#### 4.4. Process temperatures as a measure of the thermal load

In order to assess the thermal load as a function of the removal rate and the grinding wheel specification, process temperatures are measured. A comparison of different grinding wheel specifications with regard to their generated process temperatures is shown in Figure 6. The previously established hypothesis regarding the increased process heat of the tool number six with 46% porosity and tool number four with a grain concentration of C176 is confirmed. The two tools have the highest measured process temperatures in the investigated specification and parameter range. The grinding wheel number six with a porosity of 46% has a higher process temperature with a 6 mm³/mms chip removal rate than the reference tool number one with a porosity of 38% at 8 mm³/mms and otherwise the same specifications. This effect can be explained by the reduced proportion of thermally conductive bond. Although a higher porosity provides more space for cooling lubricant and chip removal, the influence of the thermal conductivity of the bonding material predominates. A similar behaviour is observed for an increase in grain concentration. The thermal conductivity of diamonds is high. In the case of increasing their concentration while maintaining the same

porosity, however, the thickness of the bond bridges in the tool decreases.

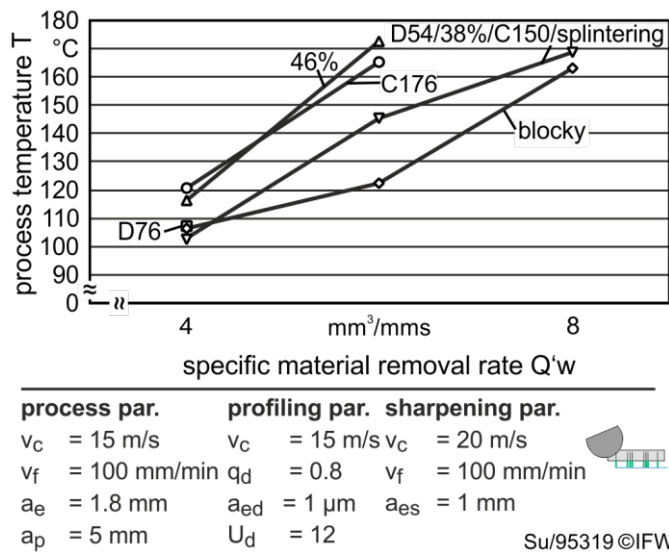


Figure 6: Influence of the grinding wheel specification on the process temperature while grinding

But they in turn distribute the heat from the contact zone on the engaging diamonds throughout the tool. This results in a reduced heat dissipation from the contact zone and consequently increased temperature in the grinding process.

#### 4.5. Analysis of the material separation in grinding

The remaining grinding wheel specifications can not be clearly distinguished with regard to their generated process heat. The grinding wheel number five with blocky grains generates lower process temperatures than the reference wheel number one with the grains that are more likely to splinter. It can be derived from the measured spindle powers and normal forces, that there is an efficient material separation. In comparison to the splintering diamond grain of the reference tool, however, a primary plowing material separation mechanism is suspected in case of the blocky grain. This type of material separation has an increased energy demand, in contrast to the separating mechanism. This is confirmed by the measured spindle load. In order to evaluate the type of material separation, quick stops of the grinding process are performed. The trial workpiece is mounted in a guided clamping device and accelerated out of the contact zone during the grinding process. The energy required for the acceleration of the workpiece is provided by a bolt gun. The gas pressure of the propellant ejects the firing pin and separates the engaging partners of the grinding process in a very short time. The speed of separation increases the cutting speed  $v_c$ . This way a snapshot of the chip formation on the workpiece surface is generated. Subsequently, scanning electron micrographs of the generated workpiece surface are made in order to evaluate the interrupted chip formation. In Figure 7 it can be seen that in the case of interrupting the machining of carbide instantaneously, no chip roots are generated, as they occur during the grinding of ductile materials such as steel and metallic alloys. Rather, different forms of burrs are detected. The created images

confirm the established hypothesis. The ratio between spindle load and normal force in case of both grain types is advantageous and the process temperatures are at a similar level.

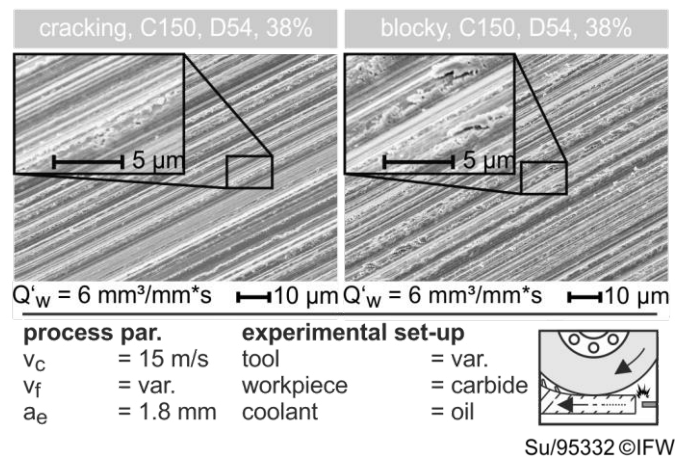


Figure 7: Chip formation during grinding of cemented carbide depending on the diamond grain type

However, the material separation in case of the likely to splinter diamond grains of the reference tool is more efficient. The scanning electron micrographs show a high level of generated burrs and brittle-hard material separation behavior in the case of blocky grains, while the generated traces of splintering diamond grains are free of these phenomena. The material separation is more efficient, which is why the spindle load, measured normal forces and process temperatures are at the lowest level of all investigated tools.

#### 4.6. Life cycle and machining efficiency increase

It is known in the state of the art that an increase of compressive residual stresses leads to a higher lifetime of the ground workpieces [18]. Figure 8 shows the measured residual stresses generated by the investigated grinding wheel specifications. All of them generate compressive stresses and except for tool number two with a grain size of  $30 \mu\text{m}$  the values are comparable with a value around  $-800 \text{ MPa}$  respectively. Residual stresses are a product of mechanical and thermal loads on the workpiece. While tool number four with a grain concentration of C176 and six with a porosity of 46% generated higher process temperatures their process forces also exceeded the values of the reference tool number one and the tool number five with embedded blocky grains. It can be summarized that the investigated porous metal bond with a grain size of  $54 \mu\text{m}$ , blocky or splintering grains, a grain concentration of C150 or C176 and a porosity of 38 or 46% generates high compressive stresses. This in turn leads to an increased life cycle of the ground workpiece. By correlating these results with the spindle load it can be found out, that the reference tool number one machines the workpiece in the most efficient way. The tool with  $54 \mu\text{m}$  splintering grains with a concentration of C100 and a porosity of 38% needs the least amount of energy to machine one volume element of cemented carbide.

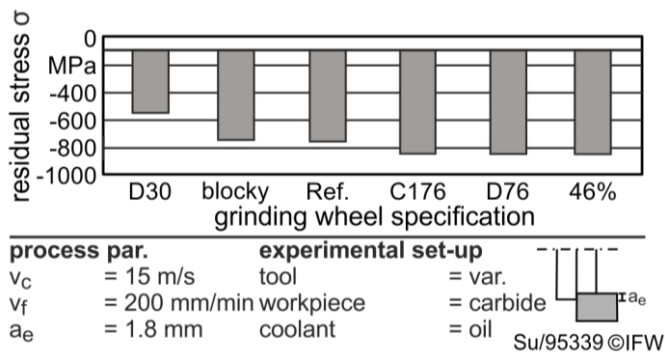


Figure 8: Generated residual stress values depending on the grinding wheel specification

## 5. Conclusion and outlook

Grinding is compared to machining processes with geometrically defined cutting edges characterized by a significantly higher energy consumption per machined volume element. In the present contribution, three methods are presented whose correlation allows for a holistic view of the energy conversion in the grinding process. The spindle power and normal force quantify the mechanical load on the engaging tool and workpiece, as well as the energy consumption for machining. The consideration of the process temperature allows an evaluation of the conversion of heat in the process. Scanning electron micrographs of workpiece surfaces generated by a quick stopping device allow for the evaluation of the material separation. The correlation of the measurement results mentioned before allows for the evaluation of the efficiency of the cutting process and the selection of the most productive wheel specification with regard to thermal and mechanical loading of the engaging partners as well as the efficiency of the material separation.

The described methodology to select grinding wheels with the most efficient material removal mechanism allows for two life cycle increase approaches. For once a decrease of thermal and mechanical workpiece load is possible while maintaining the material removal rate. Secondly the material removal rate can be increased up to a threshold value while maintaining the workpiece quality. The first approach allows for the increase of the life cycle of the workpiece. The reduced mechanical and thermal loads allow for an increase of residual compressive stresses of the ground workpiece. This, in turn leads to a higher lifetime of these workpieces. The second approach allows for the reduction of the production time in total, since the productivity can be increased. The necessary energy per part can be reduced. Additionally the machine tool is conserved since its working hours are reduced. In the next step, these findings will be transferred to the application of tool grinding and compared to the state of the art.

## Acknowledgements

The authors would like to thank the Federal Ministry for Economic Affairs and Energy (BMWi) Germany for their organizational and financial support within the project “MetScheibeII” (IGF Nr. 18826 N).

Supported by:



on the basis of a decision  
by the German Bundestag

## References

- [1] Malkin, S.; Hwang, T.W.: Grinding Mechanisms for Ceramics. CIRP Annals-Manufacturing Technology, Vol. 45(2), p. 569-580, 1996
- [2] Biermann, D.; Würz, E.: A Study of grinding silicon nitride and cemented carbide materials with diamond grinding wheels. Production Engineering Research and Development (WGP), Vol. 3, p. 411-416, 2009.
- [3] Van der Meer, M.: Bearbeitung keramischer Funktionsflächen für Knieimplantate. Dissertation, University Hannover, 2011
- [4] Denkena, B.; de Leon, L.; Wang, B.; Krawczyk, T.: Manufacturing of Riblet-Structures by Profile Grinding with Metal Bonded Wheels. Proceedings of the 10th International Conference of the European Society for Precision Engineering and Nanotechnology (euspen), Volume 2, May 31st - June 4th 2010, Delft, Netherlands, p. 295-298, 2010
- [5] Ruff, A.W.; Sin, F.; Evans, C.J.: Damage process in ceramics resulting from diamond tool indentation and scratching in various environments, Wear, Vol. 181-183, p. 551-562, 1995
- [6] Klocke, F.; König, W.: Manufacturing Processes 2 - Grinding, Honing, Lapping, Springer - Verlag, Berlin - Heidelberg, 2009
- [7] Gentzen, J.: Energieeffiziente Feinbearbeitung mit geometrisch unbestimmter Schneide und Minimalmengenschmierung, Jahrbuch Schleifen, Honen, Läppen und Polieren, Hrsg. Hoffmeister, H.W.; Denkena, B., Vol. 66, p. 111-128, 2013
- [8] Brinksmeier, E.; Heinzl, C.; Wittmann, M.: Friction, Cooling and Lubrication in Grinding, CIRP Annals, Vol. 48, Issue 2, 1999, p. 581-598
- [9] Hülsemeyer, L.: Energieeffizienz spanender Werkzeugmaschinen und bedarfsgerechter Betrieb am Beispiel der inneren Kühlschmierstoffzufuhr, Dissertation, University Hannover, 2016
- [10] Denkena, B., Köhler, J., Krawczyk, T.: Schleifen von Hartmetall mit porösen metallisch gebundenen Diamantschleifscheiben, Jahrbuch Schleifen, Honen, Läppen und Polieren, Vol. 66, p. 171-178, 2013
- [11] Wunder, S.: Verschleissverhalten von Diamantabrichtrollen beim Abrichten von Korund-Schleifschnecken, Dissertation, ETH Zürich, 2012
- [12] Carslaw, H.S.: Introduction to the Mathematical Theory of the Conduction of Heat in Solids. Second Edition, Macmillan and Co. Ltd., London, 1921
- [13] Carslaw, H.S., Jaeger, J.C.: Conduction of Heat in Solids. Oxford Science Publications, Oxford University Press, 1959
- [14] Jaeger, J.C.: Moving Sources of Heat and the Temperature at Sliding Contacts, Proceedings of the Royal Society of New South Wales, Vol. 76, p. 203-224, 1942
- [15] Götttsching, T.C.: Schleifen von aluminiumhaltigem UHC-Stahl, Dissertation, University Hannover, 2017
- [16] Takazawa, K.: Thermal Aspects of the Grinding Operation. Industrial Diamond Review, Vol. 32, 1972
- [17] Sunarto, Y, I.: Creep feed profile grinding of Ni-based superalloys with ultrafinepolycrystalline cBN abrasive grits, Precision Engineering, Vol. 25, p. 274-283, 2001
- [18] Denkena, B.; Tönshoff, H.-K.: Basics of Cutting and Abrasive Processes, Springer - Verlag, Berlin - Heidelberg, 2013